Title
Role of EPI-FLAIR in Patients with Acute Stroke: A Comparative Analysis with FLAIR

Journal
American Journal of Neuroradiology, 35(5)

ISSN
0195-6108

Authors
Meshksar, A
Villablanca, JP
Khan, R
et al.

Publication Date
2014-05-01

DOI
10.3174/ajnr.a3786

Peer reviewed

Role of EPI-FLAIR in Patients with Acute Stroke: A Comparative Analysis with FLAIR

A. Meshksar, J.P. Villablanca, R. Khan, R. Carmody, B. Coull, and K. Nael

ABSTRACT

BACKGROUND AND PURPOSE: Further improvement in acquisition speed is needed, if MR imaging is to compete with CT for evaluation of patients with acute ischemic stroke. The purpose of this study was to evaluate the feasibility of implementing an echo-planar fluid-attenuated inversion recovery (EPI-FLAIR) sequence into an acute MR stroke protocol with potential reduction in scan time and to compare the results with conventional FLAIR images.

MATERIALS AND METHODS: Fifty-two patients (28 men and 24 women; age range, 32–96 years) with acute ischemic stroke were prospectively evaluated with an acute stroke MR protocol, which included both conventional FLAIR and EPI-FLAIR imaging with integration of parallel acquisition. The image acquisition time was 52 seconds for EPI-FLAIR and 3 minutes for conventional FLAIR. FLAIR and EPI-FLAIR studies were assessed by 2 observers independently for image quality and conspicuity of hyperintensity in correlation with DWI and were rated as concordant or discordant. Coregistered FLAIR and EPI-FLAIR images were evaluated for signal intensity ratio of the DWI-positive lesion to contralateral normal white matter.

RESULTS: An estimated 96% of all FLAIR and EPI-FLAIR studies were rated of diagnostic image quality by both observers, with interobserver agreements of $\kappa = 0.82$ and $\kappa = 0.63$ for FLAIR and EPI-FLAIR, respectively. In 36 (95%) of 38 patients with acute infarction, FLAIR and EPI-FLAIR were rated concordant regarding DWI lesion. The mean ± standard deviation of the signal intensity ratio values on EPI-FLAIR and FLAIR for DWI-positive lesions were 1.28 ± 0.16 and 1.25 ± 0.17, respectively ($P = .47$), and demonstrated significant correlation ($r = 0.899$, z value $= 8.677$, $P < .0001$).

CONCLUSIONS: In patients with acute stroke, EPI-FLAIR is feasible with comparable qualitative and quantitative results to conventional FLAIR and results in reduced acquisition time.

ABBREVIATIONS: AIS = acute ischemic stroke; GRE = gradient recalled-echo; SD = standard deviation; SIR = signal intensity ratio

Neuroimaging plays a central role in the evaluation of patients with acute ischemic stroke (AIS). With improved technology during the last decade, imaging now provides information beyond the mere presence or absence of intracranial hemorrhage. Multimodal cerebrovascular CT and MR can now provide information about tissue viability, site of occlusion, and collateral status. The success of CT in the initial evaluation of AIS is due, in part, to fast acquisition time, widespread availability, and ease of interpretation in the emergency department setting.

MR imaging has been demonstrated to be more sensitive for the detection of acute ischemia and more specific for delineation of infarction core volume compared with CT.[1,2] However, because of longer acquisition time and limited availability, it has been mainly used in large institutions and comprehensive stroke centers. With recent advances in MR technology, a comprehensive MR protocol including parenchymal imaging (DWI, gradient recalled-echo [GRE], FLAIR), MRA, and MR perfusion can now be adequately obtained in 20 minutes as demonstrated in several clinical trials.[3-7] In a likewise fashion, the introduction of multisection technology has dramatically increased the speed and simplicity of CT techniques and has set a high standard for alternative imaging techniques. A comprehensive CT stroke algorithm including parenchymal imaging (noncontrast head CT), CTA, and perfusion/penumbral imaging by CT perfusion can now be ac-

Received May 10, 2013; accepted after revision September 8.

From the Departments of Medical Imaging (A.M., R.K., R.C., K.N.), and Neurology (B.C.), University of Arizona; Tucson, Arizona; and Department of Radiological Sciences (J.P.V.), University of California at Los Angeles, Los Angeles, California.

Abstract previously presented at: Annual Meeting of the American Society of Neuroradiology, May 22, 2013; San Diego, California.

Please address correspondence to Kambiz Nael, MD, Assistant Professor of Radiology, Director of Neuroradiology MRI, Department of Medical Imaging, Neuroradiology Section, University of Arizona Medical Center, 1501 N. Campbell, PO Box 245067, Tucson, AZ; e-mail: kambiz@radiology.arizona.edu

http://dx.doi.org/10.3174/ajnr.A3786

quired and processed in a comparable period.[8,9] If MR imaging is to compete with CT for evaluation of acute stroke, there is need for further improvements in acquisition speed.

FLAIR imaging as a part of an acute MR stroke protocol has several advantages including detection of subtle cerebral subarachnoid hemorrhage; added diagnostic value to GRE images for the detection of intra-arterial clot[10-12]; and, most important, helping to determine the age of infarction in patients with both known and unknown time of onset of neurologic deficit (wake-up stroke).[13] The latter advantage has a major impact on the treatment planning because FLAIR hyperintensity is usually indicative of a completed stroke, thereby excluding these patients from most therapeutic interventions.[14,15]

Introduction of fast imaging techniques such as parallel acquisition[16] and EPI[17,18] has significantly enhanced the performance of MR imaging in acquisition speed. The main advantage of EPI, as in the case of DWI, is rapid acquisition time, which is made possible by rapid gradient switching, which allows the acquisition of all frequency and phase-encoding steps during a single pulse cycle. The addition of parallel imaging can further enhance the acquisition speed and may also serve to mitigate the geometric distortion and susceptibility artifacts commonly associated with long echo-train sequences such as EPI.[19,20] If their potential is realized, the application of EPI and parallel imaging techniques to the FLAIR sequence can result in a reduction of image acquisition time of the entire brain to less than a minute, a 3-fold reduction in scan time compared with conventional FLAIR imaging. The purpose of this study was to evaluate the feasibility of implementing an EPI-FLAIR sequence into an acute MR stroke protocol with its potential reduction in scan time, and to compare the result with conventional FLAIR imaging.

MATERIALS AND METHODS

This prospective study was conducted between May and September 2012. All examinations were performed in accordance with institutional review board guidelines with an approved study protocol. Our inclusion criteria included 1) patients with clinical suspicion of AIS who presented within the first 24 hours from the onset of neurologic deficits, and 2) acquisition of MR imaging as the initial imaging study. Exclusion criteria included ferromagnetic or MR incompatible implants, glomerular filtration rate < 30 mL/min/1.73 m^2, and severe claustrophobia. The baseline NIHSS scores and median time from stroke onset to MR imaging were documented for each patient when available.

Image Acquisition

All patients were studied on a 1.5T MR system (Avanto; Siemens, Erlangen, Germany). The imaging protocol included DWI, conventional FLAIR, EPI-FLAIR, GRE, MRA, and dynamic susceptibility contrast perfusion imaging. A combination of head and neck coil with up to 12 channels was used for radiofrequency signal reception. A spin-echo and an EPI sequence were used for FLAIR and EPI-FLAIR, respectively, with the following parameters: TR, 9000 ms (10,000 ms for EPI-FLAIR); TE, 88 ms (106 ms for EPI-FLAIR); inversion time, 2500 ms; flip angle, 150° (90° for EPI-FLAIR). Other imaging parameters, including field of view of 22 cm, matrix size of 256 mm (192 mm for EPI-FLAIR), and 26 total sections each 5-mm thick, were kept constant between the 2 sequences. Integration of generalized autocalibrating partially parallel acquisition with an acceleration factor of 2 resulted in an acquisition time of 3 minutes for conventional FLAIR and 52 seconds for EPI-FLAIR, respectively.

Image Analysis

Conventional FLAIR and EPI-FLAIR images were reviewed independently by 2 experienced neuroradiologists and in separate reading sessions. The observers were able to adjust image contrast and size. A 4-scale imaging score was used to evaluate the image quality with respect to susceptibility-mediated distortion at tissue interfaces, noise, and motion: 1) poor image quality, not interpretable; 2) impaired image quality with significant distortion and noise, limiting delineation of major structures; 3) good image quality with minimal distortion, diagnostic image quality; and 4) excellent image quality with delineation of all structures.

In addition to image quality, the observers were asked to correlate the FLAIR and EPI-FLAIR images with DWI-ADC maps, determine the presence of hyperintense signal corresponding to the area of restricted diffusion, and categorize the image pairs as concordant or discordant. This comparison was performed during different reading sessions for both conventional FLAIR and EPI-FLAIR, to avoid recall bias. The observers were also asked to localize the FLAIR/EPI-FLAIR lesions to 3 anatomic regions: 1) supratentorial, 2) infratentorial, or 3) both. Finally, and again in a different reading session, any discrepancy between readers for lesion location or FLAIR/EPI-FLAIR DWI correlation was resolved by consensus agreement. These scores were then used to perform comparative analysis between conventional FLAIR and EPI-FLAIR.

DWI, FLAIR, and EPI-FLAIR images for each patient were coregistered by a commercially available FDA-approved software (Olea Sphere; Olea Medical SAS, La Ciotat, France) by use of a 12 degrees-of-freedom transformation and a mutual information cost function. This was followed by visual inspection to ensure adequate alignment. The segmentation was performed by a single neuroradiologist. The ROIs were placed over the region of infarction (DWI+) in 1 section to extract the corresponding FLAIR and EPI-FLAIR signal intensity values. ROIs were then mirrored onto the contralateral hemisphere, and the SIR values with respect to contralateral, normal-appearing white matter were calculated by use of the mean SI values. Manual restriction of the ROIs was applied when necessary to avoid regions with prior infarction or chronic microvascular ischemic changes.

In patients who did not have a DWI abnormality, a 1-cm ROI was placed in the centrum semiovale and automatically mirrored onto the contralateral hemisphere to calculate the SIR.

The volume of lesions on FLAIR and EPI-FLAIR studies was calculated by use of Olea Sphere software. ROIs were created on the basis of the signal intensity subsuming the entire region of hyperintensity, and the volume and standard deviation (SD) was calculated. The range included was the interval of pixel values to

Table 1: Correlation of FLAIR and EPI-FLAIR compared with DWI ($n = 50$)

N	DWI	FLAIR (Signal)	EPI-FLAIR (Signal)	Conclusion
12	−	−	−	No ischemic infarction
10	+	−	−	Concordant FLAIR–EPI-FLAIR, early stage of ischemic infarction
26	+	+	+	Concordant FLAIR–EPI-FLAIR, completed infarction
2	+	+	−	EPI-FLAIR discordant with FLAIR

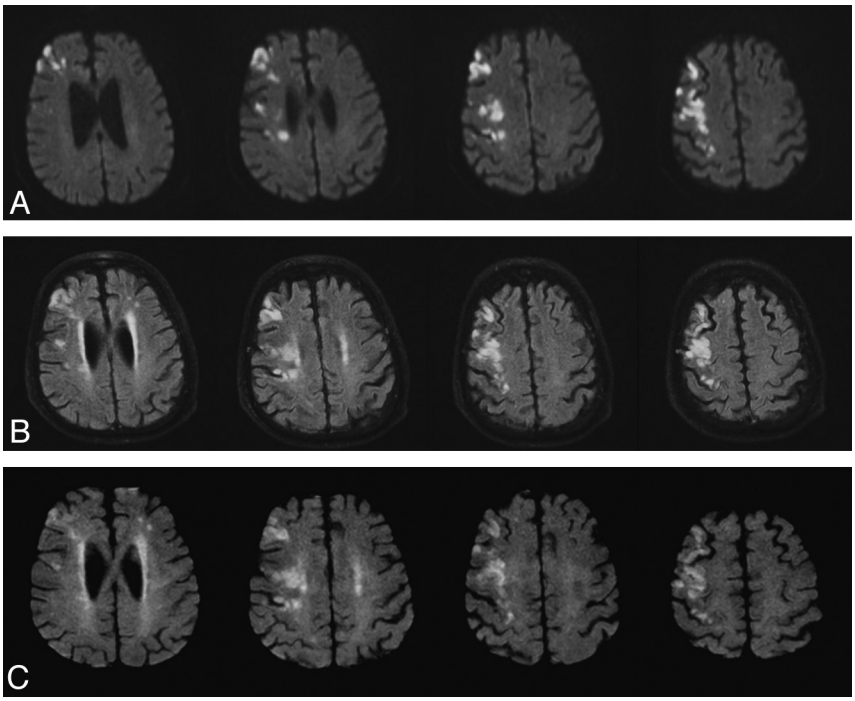

FIG 1. An 86-year-old man with acute onset left-sided weakness after elective cardiac surgery, NIHSS:8. Axial DWI (4500/90, $b = 1000$ s/mm^2) (*A*), FLAIR (9000/88/2500) (*B*), and EPI-FLAIR (10,000/106/2500) (*C*) images obtained 4.5 hours after the onset of symptoms. Watershed infarctions are noted along the right cerebral hemisphere deep white matter zones. Note the comparable image quality between FLAIR and EPI-FLAIR, both demonstrating increased signal intensity in the region of DWI abnormality, indicative of completed infarctions. Acquisition time for FLAIR was 3 minutes; for EPI-FLAIR, it was 52 seconds.

include the central value of the initial seed-voxel. Manual restriction of the ROIs was applied when necessary. The largest lesion in a single section was selected for the volume measurement. For patients with multiple or embolic infarction, the largest lesion was selected for volume analysis.

Finally, the patients with acute infarction were categorized in 2 groups based on time from onset to MR imaging of ≥4.5 hours as the cutoff value for thrombolysis. The mean ± SD of the SIR values on EPI-FLAIR and FLAIR correlated in these 2 groups.

Statistical Analysis

Statistical analysis was performed by use of MedCalc Version 12.2.1 (MedCalc Software, Mariakerke, Belgium).The Wilcoxon signed rank test was used to compare the mean ratings of FLAIR and EPI-FLAIR. A weighted κ test with a calculation of 95% CI was used to evaluate the interobserver and intermodality agreement. The Spearman correlation coefficient was calculated for the comparative analysis of DWI with FLAIR/EPI-FLAIR. The quantitative SIR values between FLAIR and EPI-FLAIR were tested with a *t* test and a correlation coefficient (*r*). The significance level was defined as $P < .05$ (2-sided).

RESULTS

A total of 52 consecutive patients (28 men and 24 women; age range, 32–96 years) met our inclusion criteria. The median and interquartile ranges of the baseline NIHSS scores were 11 and 10.75, respectively. The median and interquartile ranges of the time from presentation to MR imaging was 6 and 7.5 hours, respectively, in 34 of 38 patients with acute ischemic infarction. In 4 patients with acute infarction, the time from the onset of symptoms was unknown.

Two studies (4%) were deemed nondiagnostic and were excluded from the study, one because of susceptibility artifacts caused by dental braces and the other because of significant motion artifacts. In 50 (96%) of 52 studies, FLAIR and EPI-FLAIR studies were rated of diagnostic image quality (image quality ≥3) by both observers. The median and ranges of image quality scores were 4 and 3–4, respectively, for FLAIR by both observers, with no statistically significant difference ($P = .54$) and with an interobserver agreement of $\kappa = 0.82$; 95% CI, 0.67–0.90. The median and ranges of image quality scores were 3 and 3–4, respectively, for EPI-FLAIR by both observers with no statistically significant difference ($P = .4$) and an interobserver agreement of $\kappa = 0.63$ (95% CI, 0.37–0.80).

Twelve patients did not have restricted diffusion on DWI; therefore, results were negative on both FLAIR and EPI-FLAIR with complete concordance. There were 38 patients who had acute infarction (+DWI lesion). The infarctions were supratentorial in 32 patients, infratentorial in 2 patients, and both supratentorial and infratentorial in 4 patients. In 36 (95%) of 38 patients with acute infarction, FLAIR and EPI-FLAIR concurred and demonstrated good correlation: $r = 0.88$; 95% CI, 0.80–0.93 (Table 1). In 26 patients in whom both FLAIR and EPI-FLAIR were positively concordant with DWI (Fig 1), the time from onset to MR imaging ranged from 2.5–18 hours. In 10 patients for whom both FLAIR and EPI-FLAIR were negatively concordant with DWI hyperintensity, the time from presentation to MR imaging ranged from 50 minutes to 3 hours. In only 2 patients (5%), EPI-FLAIR was discordant with FLAIR and was unable to show subtle FLAIR hyperintensity corresponding to a DWI lesion. In 1 case, there was a punctate small thalamic infarction. The other discordant case was a hyperacute ischemic infarction in a patient who

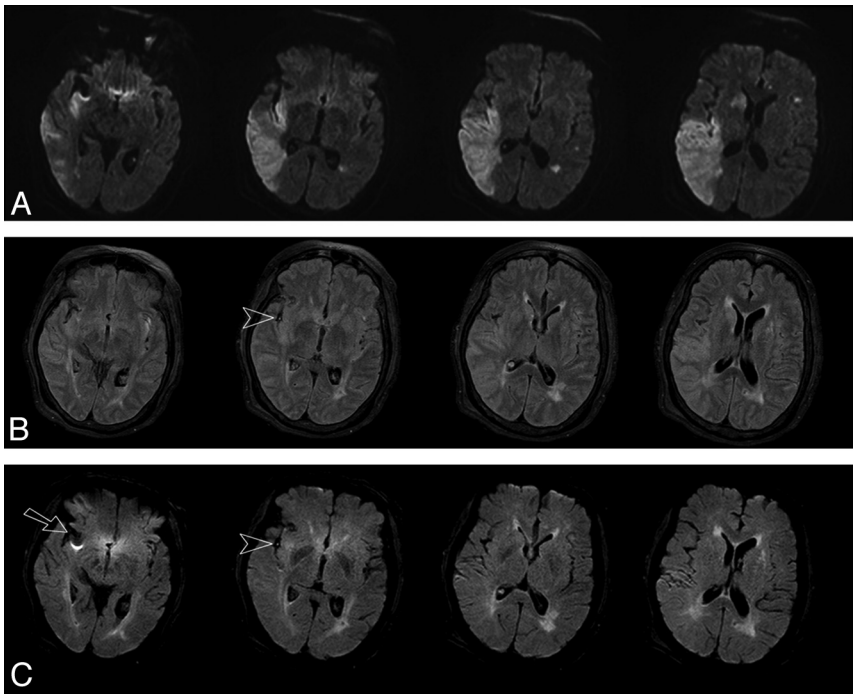

FIG 2. A 60-year-old man with sudden-onset left-sided weakness after an aneurysm coil was placed for a proximal supraclinoid ICA aneurysm. Axial DWI (4500/90, b = 1000 s/mm^2) (*A*), FLAIR (9000/88/2500) (*B*), and EPI-FLAIR (10,000/106/2500) (*C*) obtained approximately 60 minutes after onset of symptoms. Acute infarction along the right MCA territory is noted. The signal intensity ratio of the lesion to the contralateral hemisphere was elevated and measured 1.19 for FLAIR and 1.15 for EPI-FLAIR. Qualitatively, however, very subtle increased hyperintensity corresponding to the region of DWI abnormality is evident on FLAIR but is not clearly seen on EPI-FLAIR. Note the susceptibility artifacts related to the dislodged coil in the MCA bifurcation, which is more pronounced on EPI-FLAIR (*arrow*) and likely contributed to field inhomogeneity and may have explained the qualitative discrepancy with FLAIR. Note the hyperintense vessel sign (*arrowheads*) on both FLAIR and EPI-FLAIR caused by sluggish flow or clot in the sylvian MCA branches.

Table 2: Comparison of SIR values between FLAIR and EPI-FLAIR studies (n = 50)

	FLAIR SIR	EPI-FLAIR SIR	*T* Test (*P* Value)
DWI negative			
(−) FLAIR, (−) EPI-FLAIR (n = 12)	1.02 ± 0.005	1.02 ± 0.006	.2
DWI positive			
<4.5 hours of time from onset to MR imaging (n = 12)	1.14 ± 0.08	1.10 ± 0.06	.22
>4.5 hours of time from onset to MR imaging (n = 22)	1.36 ± 0.16	1.33 ± 0.17	.83
(+) FLAIR, (−) EPI-FLAIR (n = 2)	1.15 ± 0.03	1.13 ± 0.05	/A[a]

Note:—Data are mean ± standard deviation.

[a] In 2 discrepant cases, the SIR values were comparable. The sample was too small for evaluation with the *t* test. In 4 patients with unknown time of presentation, the SIR values were concordant between FLAIR and EPI-FLAIR (SIR > 1.3, n = 3; SIR < 1.3, n = 1).

underwent imaging only 1 hour after endovascular aneurysm coiling (Fig 2). There were no discrepancies between FLAIR and EPI-FLAIR in identification of the anatomic location of infarctions. A hyperintense vascular sign, which was suggestive of a blood clot or sluggish flow, was identified in 5 cases on both FLAIR and EPI-FLAIR (supraclinoid internal carotid artery [n = 2], basilar artery [n = 1], and proximal MCA [n = 2]).

The volume (mean ± SD) of lesions on FLAIR and EPI-FLAIR were 15.4 ± 12.7 and 17.5 ± 15.8, respectively (P = .3).The mean ± SD of the SIR values for EPI-FLAIR and FLAIR are detailed in Table 2. In 12 patients with no infarction, the mean SIR values were 1.02 for both FLAIR and EPI-FLAIR (P = .2). The overall mean ± SD of the SIR values on EPI-FLAIR and FLAIR for DWI-positive lesions were 1.28 ± 0.16 and 1.25 ± 0.17, respectively (P = .47).

The mean (1.33) of EPI-FLAIR SIR values for patients who presented > 4.5 hours from the onset was statistically higher (t value, 7.959; P < .0001) than for those who presented < 4.5 hours from the onset (1.10). In a similar fashion, the mean (1.36) of FLAIR SIR values for patients who presented > 4.5 hours from the onset was statistically higher (t value, 7.491; P < .0001) than for those who presented < 4.5 hours (1.14).

There was significant correlation for the SIR values between FLAIR and EPI-FLAIR (r = 0.899; z value = 8.677; P < .0001). Fig 3 shows the scatterplots and Bland-Altman plots of the SIR between FLAIR and EPI-FLAIR. In 2 discordant cases, despite visual discordancy between FLAIR and EPI-FLAIR for the detection of hyperintensity corresponding to a DWI lesion, the SIR values were comparable (Table 2). In 4 patients with an unknown time of presentation, the FLAIR and EPI-FLAIR values were concordant, with SIR values > 1.3 in 3 patients and SIR < 1.3 in 1 patient.

DISCUSSION

There are 2 different schools of thought on neuroimaging for AIS. Although CT is the most widely available method and is a faster imaging technique, some larger institutions and many comprehensive stroke centers favor streamlined MR protocols compared with CT in the acute stroke setting because of the higher specificity and superior tissue characterization afforded by MR imaging.

Our results demonstrate that the described EPI-FLAIR sequence is feasible for use in the acute stroke setting, with comparable qualitative and quantitative results to a conventional FLAIR sequence, and has the potential for saving valuable acquisition time in patients with AIS. For such patients within the therapeutic time window, it has been estimated that for every minute during which ischemic stroke is left untreated, approximately 1.9 million neurons are lost.[21] Therefore, an interest prevails in enhancing image acquisition and postprocessing speed for both CT- and MR-based imaging protocols, with the goal of identifying the optimal balance between the concepts of "time is brain" and "imaging is brain."[22,23]

The MR imaging treatment scheme for AIS at our institution includes a rapid imaging plan including DWI, GRE, and FLAIR.

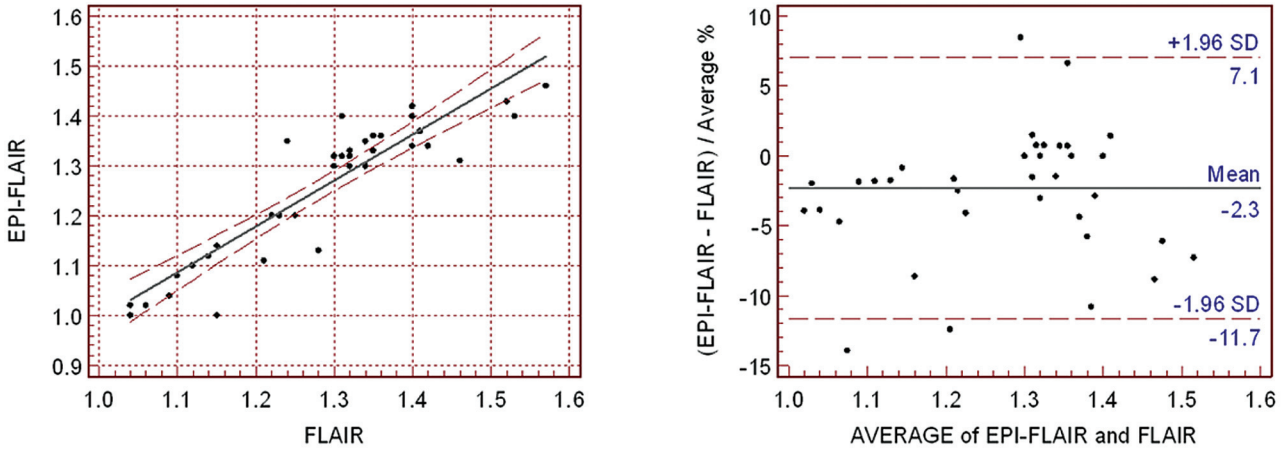

FIG 3. Bland-Altman plots and scatterplot show significant correlation ($r = 0.899$; z value $= 8.677$; $P < .0001$) for the SIR values between FLAIR and EPI-FLAIR in patients with acute infarction (DWI-positive lesions [$n = 38$]).

The images are then reviewed by neuroradiologists and neurologists on-line. On the basis of clinical deficits and imaging findings, a decision is made to give or withhold thrombolysis by IV tPA. It should be noted that saving 2 minutes of acquisition time is a step forward in improved total MR image time. This is particularly relevant because the time reduction occurs before the thrombolysis decision point in our imaging treatment scheme.

In general, magnetic field inhomogeneity and susceptibility artifacts are problematic for imaging sequences such as EPI, because of long acquisition intervals and long echo trains.[17] As a consequence, prior reports on the use of EPI-FLAIR sequences to evaluate intracranial processes such as brain tumors[24,25] and stroke[26] have produced mixed results, with susceptibility artifacts being a major limiting factor. We postulate that the improved image quality of our EPI-FLAIR technique can be partly explained by the integration of parallel imaging and its complementary effects with EPI.

Parallel imaging results in faster acquisition speed and also helps to mitigate the distortion and susceptibility artifacts associated with the EPI technique.[19,20] Integration of parallel imaging with the EPI sequence and undersampling of *k*-space can result in shortening of the echo-train length and an increase in blip gradients. Accordingly, the pixel bandwidth in the phase-encoding direction increases, which leads to a reduction in susceptibility artifacts. In addition, the shortened echo train provides the opportunity to reduce the echo time and hence the T2 decay, which in turn can lead to a significant SNR gain, offsetting the SNR penalty incurred by use of the parallel imaging technique. In this study, the complementary effects of integration of parallel imaging with EPI has resulted in a FLAIR sequence with diagnostic image quality that avoids the potential EPI-related susceptibility artifacts, when compared with conventional FLAIR.

The main clinical use of FLAIR imaging in the setting of acute stroke is to identify acute ischemic infarcts within the thrombolytic time window. Use of only time from symptom onset can result in exclusion of potentially treatable ischemic stroke cases when the time of onset is uncertain, such as patients with symptoms first noted on awakening, or those with unwitnessed onset, who are unable to provide an accurate history. As a rule, the prevalence of lesion visibility on FLAIR increases as time passes from the stroke onset. Recent reports have demonstrated that approximately 27%–50% of patients with stroke have positive FLAIR findings within 3 hours and 93% at $>$ 6 hours,[13-14,27] indicating the development of cytotoxic edema, and corresponding to completed tissue infarction. Although our study goals did not include the aging of infarcts, we found that the described EPI-FLAIR sequence is comparable to conventional FLAIR in the detection of FLAIR hyperintensity corresponding to DWI abnormality, agreeing with conventional FLAIR in 92% of patients with AIS.

It is more important to note that our results indicate that the SIR values of the EPI-FLAIR technique are concordant with FLAIR in patients with time of onset to MR imaging of $<$ 4.5 hours, an important timeline for IV thrombolysis treatment planning. Our values are concordant with the results of a recently published clinical trial by Song et al.[28]

In 2 cases, EPI-FLAIR was unable to show subtle FLAIR hyperintensity corresponding to the area of infarction. However, the SIR values of these lesions were comparable (Table 2). In 1 case, the infarction was too small. The other discrepant case was a hyperacute infarction that occurred approximately 1 hour after aneurysm coil placement and consequently had very subtle FLAIR hyperintensity (Fig 2). In addition, the aneurysm coil mass in the MCA bifurcation near the vicinity of the infarction probably resulted in added susceptibility artifacts and may have caused incomplete water suppression, hence reduced lesion to background contrast ratio and a decrease in sensitivity of EPI-FLAIR. It is important to note that the SIR values of these lesions were comparable on both FLAIR and EPI-FLAIR (Table 2), suggesting that the detection of a hyperintense signal may be a null point for practical purposes if the SIR values are comparable.

This study had several limitations. The first was a relatively small sample size possibly introducing a size selection bias. The second limitation was the inherent susceptibility artifacts associated with EPI techniques. Although susceptibility artifacts were mitigated by integration of parallel imaging and did not affect the diagnostic image quality of our study, we anticipate that this could be more problematic at higher magnetic fields such as 3T, especially at tissue interfaces and near the skull base. Third, we noted

that the EPI-FLAIR sequence exhibits a reduced white-gray matter contrast ratio, likely caused by incomplete, or inhomogeneous, water suppression. This could diminish the conspicuity of the EPI-FLAIR sequence to small white matter abnormalities, a possibility not specifically addressed in our study. Larger clinical studies will likely be needed to more fully determine the clinical usefulness of the described EPI-FLAIR technique in a broader setting.

CONCLUSIONS

The described EPI-FLAIR technique is feasible, with comparable qualitative and quantitative results to conventional FLAIR images for evaluation of patients with AIS. EPI-FLAIR can be implemented in the acute stroke MR protocol, resulting in a valuable reduction in scan time.

REFERENCES

1. Jauch EC, Saver JL, Adams HP Jr, et al. **Guidelines for the early management of patients with acute ischemic stroke: a guideline for healthcare professionals from the American Heart Association/American Stroke Association.** *Stroke* 2013;44:870–947
2. Chalela JA, Kidwell CS, Nentwich LM, et al. **Magnetic resonance imaging and computed tomography in emergency assessment of patients with suspected acute stroke: a prospective comparison.** *Lancet* 2007;369:293–98
3. Kang DW, Chalela JA, Dunn W, et al. **MRI screening before standard tissue plasminogen activator therapy is feasible and safe.** *Stroke* 2005;36:1939–43
4. Hjort N, Butcher K, Davis SM, et al. **Magnetic resonance imaging criteria for thrombolysis in acute cerebral infarct.** *Stroke* 2005;36:388–97
5. Schellinger PD, Jansen O, Fiebach JB, et al. **A standardized MRI stroke protocol: comparison with CT in hyperacute intracerebral hemorrhage.** *Stroke* 1999;30:765–68
6. Albers GW, Thijs VN, Wechsler L, et al. **Magnetic resonance imaging profiles predict clinical response to early reperfusion: the diffusion and perfusion imaging evaluation for understanding stroke evolution (DEFUSE) study.** *Ann Neurol* 2006;60:508–17
7. Davis SM, Donnan GA, Parsons MW, et al. **Effects of alteplase beyond 3 h after stroke in the Echoplanar Imaging Thrombolytic Evaluation Trial (EPITHET): a placebo-controlled randomised trial.** *Lancet Neurol* 2008;7:299–309
8. Zhu G, Michel P, Aghaebrahim A, et al. **Computed tomography workup of patients suspected of acute ischemic stroke: perfusion computed tomography adds value compared with clinical evaluation, noncontrast computed tomography, and computed tomography angiogram in terms of predicting outcome.** *Stroke* 2013;44:1049–55
9. Schaefer PW, Roccatagliata L, Ledezma C, et al. **First-pass quantitative CT perfusion identifies thresholds for salvageable penumbra in acute stroke patients treated with intra-arterial therapy.** *AJNR Am J Neuroradiol* 2006;27:20–25
10. Flacke S, Urbach H, Keller E, et al. **Middle cerebral artery (MCA) susceptibility sign at susceptibility-based perfusion MR imaging: clinical importance and comparison with hyperdense MCA sign at CT.** *Radiology* 2000;215:476–82
11. Assouline E, Benziane K, Reizine D, et al. **Intra-arterial thrombus visualized on T2* gradient echo imaging in acute ischemic stroke.** *Cerebrovasc Dis* 2005;20:6–11
12. Noguchi K, Ogawa T, Seto H, et al. **Subacute and chronic subarachnoid hemorrhage: diagnosis with fluid-attenuated inversion-recovery MR imaging.** *Radiology* 1997;203:257–62
13. Thomalla G, Rossbach P, Rosenkranz M, et al. **Negative fluid-attenuated inversion recovery imaging identifies acute ischemic stroke at 3 hours or less.** *Ann Neurol* 2009;65:724–32
14. Thomalla G, Cheng B, Ebinger M, et al. **DWI-FLAIR mismatch for the identification of patients with acute ischaemic stroke within 4.5 h of symptom onset (pre-FLAIR): a multicentre observational study.** *Lancet Neurol* 2011;10:978–86
15. Aoki J, Kimura K, Iguchi Y, et al. **FLAIR can estimate the onset time in acute ischemic stroke patients.** *J Neurol Sci* 2010;293:39–44
16. Griswold MA, Jakob PM, Heidemann RM, et al. **Generalized autocalibrating partially parallel acquisitions (GRAPPA).** *Magn Reson Med* 2002;47:1202–10
17. Mansfield P. **Real-time echo-planar imaging by NMR.** *Brit Med Bull* 1984;40:187–90
18. DeLaPaz RL. **Echo-planar imaging.** *Radiographics* 1994;14:1045–58
19. Pruessmann KP. **Parallel imaging at high field strength: synergies and joint potential.** *Top Magn Reson Imaging* 2004;15:237–44
20. Wiesinger F, Van de Moortele PF, Adriany G, et al. **Potential and feasibility of parallel MRI at high field.** *NMR Biomed* 2006;19:368–78
21. Saver JL. **Time is brain–quantified.** *Stroke* 2006;37:263–66
22. Michel P, Bogousslavsky J. **Penumbra is brain: no excuse not to perfuse.** *Ann Neurol* 2005;58:661–63
23. González RG. **Imaging-guided acute ischemic stroke therapy: from "time is brain" to "physiology is brain".** *AJNR Am J Neuroradiol* 2006;27:728–35
24. Tomura N, Kato K, Takahashi S, et al. **Multi-shot echo-planar FLAIR imaging of brain tumors: comparison of spin-echo T1-weighted, fast spin-echo T2-weighted, and fast spin-echo FLAIR imaging.** *Comput Med Imaging Graph* 2002;26:65–72
25. Korogi Y, Sugahara T, Shigematsu Y, et al. **Ultrafast FLAIR imaging with single-shot echo-planar technique in evaluation of intracranial lesions.** *Comput Med Imaging Graph* 1999;23:119–26
26. Matoba M, Tonami H, Yokota H, et al. [**Echo-planar FLAIR imaging in patients with brain disorders: comparative studies with turbo-SE T2WI and turbo-FLAIR**]. [in Japanese] *Nihon Igaku Hoshasen Gakkai Zasshi* 1998;58:129–36
27. Petkova M, Rodrigo S, Lamy C, et al. **MR imaging helps predict time from symptom onset in patients with acute stroke: implications for patients with unknown onset time.** *Radiology* 2010;257:782–92
28. Song SS, Latour LL, Ritter CH, et al. **A pragmatic approach using magnetic resonance imaging to treat ischemic strokes of unknown onset time in a thrombolytic trial.** *Stroke* 2012;43:2331–35